

NO Adsorption and Dissociation on Rh(111): PM-IRAS Study

W. T. Wallace, Y. Cai, M. S. Chen, and D. W. Goodman*

Department of Chemistry, P.O. Box 30012, Texas A&M University, College Station, Texas 77842-3012

Received: December 7, 2005; In Final Form: February 6, 2006

We have used in situ polarization-modulation infrared reflection absorption spectroscopy to study the adsorption/dissociation of NO on Rh(111). While these studies have not been conclusive regarding the detailed surface structures formed during adsorption, they have provided important new information on the dissociation of NO on Rh(111). At moderate pressures ($\leq 10^{-6}$ Torr) and temperatures (< 275 K), a transition from 3-fold hollow to atop bonding is apparent. Data indicate that this transition is not due to the migration of the 3-fold hollow NO but rather to the adsorption of gas-phase NO that is directed toward the atop position due to the presence of NO decomposition products, particularly chemisorbed atomic O species at the hollow sites. These results indicate that NO dissociation occurs at temperatures well below the temperature previously reported. Additionally, high pressure (1 Torr) NO exposure at 300 K results in only atop NO, calling into question the surface structures previously proposed at these adsorption conditions consisting of atop and 3-fold hollow sites.

Introduction

Because of its ability to convert NO to N_2 with high selectivity, rhodium has become an integral part of automotive catalytic converters.^{1–4} To gain a better understanding of the mechanism behind this conversion, numerous surface science studies have been carried out using techniques such as low-energy electron diffraction (LEED), temperature programmed desorption (TPD), X-ray photoelectron spectroscopy (XPS), and high-resolution electron energy loss spectroscopy (HREELS). These studies have generally focused on the adsorption and dissociation that take place on the low Miller index surfaces (i.e., Rh(111), (100), and (110)) and also on polycrystalline Rh.^{5–13} However, more recent work has focused on the more highly stepped surfaces in an attempt to determine if these surfaces are more active for NO dissociation than flat surfaces.^{14–16}

Early work on the NO/Rh(111) system was carried out by Castner et al. using LEED and TPD.^{17–19} These authors found that NO adsorbed at 298 K produced a $c(4 \times 2)$ LEED pattern at low coverage (i.e. ~ 0.1 langmuir, $1 \text{ L} = 1 \times 10^{-6}$ Torr s), which converted to a (2×2) pattern as the NO coverage was increased beyond 1 L. Subsequent studies aimed at understanding NO coordination and dissociation on the Rh(111) system were carried out by Root et al. using TPD and HREELS.^{20–22} At low NO coverages at 95 K, these authors observed a loss feature between 1480 and 1630 cm^{-1} that was attributed to NO bound at bridging sites. They also noted that no LEED pattern was observed at 95 K but that heating to 250 K resulted in the appearance of a (2×1) pattern, in contrast to the patterns seen by Castner et al.¹⁷ TPD showed desorption of NO at ~ 450 K, with N_2 and O_2 desorbing at higher temperatures. HREELS was used to observe the dissociation of NO in situ. At low NO coverage, the NO stretching feature at 1500 cm^{-1} disappeared at 325 K, well below the NO desorption temperature, providing evidence for complete NO dissociation.

By increasing the NO coverage, the molecular NO stretching feature (1630 cm^{-1}) was still evident at 425 K, indicating that, at high coverages, dissociation is limited in the absence of NO desorption due to insufficient surface sites. The oxygen atoms produced during NO decomposition were postulated to adsorb in the hollow sites, while it was suggested that the N atoms may diffuse into the near-surface metal region. The latter conclusion followed because of the absence of a Rh–N stretching mode and the very weak N(1s) XPS intensity even at high coverages.^{15,20} Root et al. also studied the effects of coadsorbed oxygen on NO adsorption.²² After creating a surface containing 0.37 ML oxygen, exposures of small amounts of NO produced a loss peak at 1580 cm^{-1} , significantly blue-shifted from that seen when NO was exposed to the clean Rh surface. Of greater interest was the appearance of a small loss peak at 1850 cm^{-1} corresponding to NO on atop sites. Because this feature was present only with coadsorbed oxygen, the authors concluded that NO adsorbs at atop sites on Rh(111) only in the presence of coadsorbed oxygen.

More recently, Rider et al. have studied the effects of higher pressures on the surface structures obtained for NO/Rh(111).^{23,24} Using high-pressure scanning tunneling microscopy at room temperature, these authors observed a change in the NO surface structure as a function of pressure. While a (2×2) structure is obtained when small amounts of NO are added to the Rh(111) surface at 200 K, it is also possible to maintain this structure at room temperature in a background of 10^{-8} Torr. Rider et al. found that this structure transformed into (3×3) domains at ~ 300 K as the pressure was increased to 0.01–0.05 Torr. Using their pressure and temperature data, Rider et al. found that the energy barrier for the transition between the phases was on the order of 0.7 eV. Subsequent studies addressing CO and NO coadsorption found that CO and NO mixed in a (2×2) – $3(\text{CO} - \text{NO})$ structure. As the pressure of NO was increased, however, NO-rich islands formed with a (3×3) structure.

The current consensus regarding the NO/Rh(111) system can be summarized as follows. At temperatures below 275 K, NO adsorbs molecularly; above this temperature, dissociation of NO

* To whom correspondence should be addressed. E-mail: goodman@mail.chem.tamu.edu.

takes place forming two different structures that depend on the temperature and coverage. At low coverages (<0.25 ML), all NO dissociates between 275 and 325 K, and the N atoms combine and desorb between 450 and 650 K. At higher coverages, some NO dissociates above 300 K until all empty 3-fold hollow sites are filled. At this point, decomposition is inhibited. Raising the NO coverage even further results in the adsorption of NO on atop and 3-fold hollow sites. At this point, NO dissociation is inhibited until >400 K where 3-fold hollow NO begins to desorb.

While a significant number of studies has been carried out on Rh single crystals in an attempt to gain a better understanding of the mechanism of NO decomposition and the changes that occur under more realistic pressures,^{1–8,10,11,14,15,17–25} several theoretical studies of this system have also been performed.^{16,26–29} Sautet and co-workers used density functional theory (DFT) to study the adsorption of NO on Rh(111) at three different coverages.^{16,26} These authors found that at 0.33 and 0.5 ML, the most stable adsorption site for NO was a 3-fold hollow site. At 0.75 monolayers, however, the most stable configuration consisted of one NO in an atop site and two in 3-fold hollow sites. This result is in direct contrast to earlier experimental work showing NO in bridging sites^{21,22} or one NO in an atop site and two in bridging sites.¹⁸ It was later agreed following further experimental studies that the feature attributed to a bridging site was actually a 3-fold hollow site.^{5,29}

Loffreda et al.¹⁶ have used DFT to study NO adsorption on close-packed (111), open (100), and stepped (511) Rh surfaces to understand what role surface structure might play in dissociation activity. This kind of study is very relevant since the supported Rh clusters used as commercial catalysts typically exhibit a variety of surface defects. The authors found that the most stable adsorption site for NO at $1/6$ ML coverage on Rh(511) was at a bridging site overlooking a step, although several other configurations are within a few tenths of an electronvolt as stable. Regarding the dissociation of NO, the authors found the highest activity for $\langle 100 \rangle$ terraces of the Rh(511) surface and proposed that NO dissociation on Rh(111) surfaces could be dominated by steps, possibly of the $\langle 100 \rangle$ variety.

While experimental and theoretical studies on single crystal rhodium surfaces have provided a better understanding of the mechanism of NO bond scission, the ultimate goal is to determine whether the NO dissociation mechanism on single crystal surfaces is the same as that on supported metal clusters of commercial catalysts. Several groups are currently looking at various reactions involving NO on supported Rh particles.^{30–33} With respect to the question of NO decomposition, Overbury and co-workers have recently presented some intriguing results.^{30,31} These authors found that Rh supported on a reduced ceria (CeO_x) thin film is more active for NO dissociation than Rh supported on an oxidized ceria (CeO_2) thin film, which behaves like a single crystal surface. They noted that, while oxygen spillover from the Rh clusters to the support frees up sites for further NO dissociation, the level of enhanced dissociation does not appear to result simply from oxygen spillover. Using angle-resolved temperature-programmed desorption (AR-TPD), Matsushima et al.³⁴ proposed that N_2O is the reaction intermediate during NO decomposition.

In further studies, Overbury and co-workers³⁰ studied the coverage dependence of NO dissociation over Rh supported on ceria thin films. Using XPS, they found that saturation NO on Rh/ CeO_2 at 250 K results in two features in the N(1s) region, which they assigned to undissociated NO and the dissociation

product N. A Rh/ CeO_x surface was found to dissociate large amounts of NO at 300 K, with complete conversion by 350 K, while no NO dissociation was seen on the highly oxidized surface. At lower coverages, the dissociation temperature decreased for both supports. Poisoning the oxygen vacancies of the reduced ceria surface with H_2O did not affect the enhanced dissociation, supporting the previous conclusion that oxygen spillover could not account for the enhancement. The authors noted that NO dissociation had been seen at lower temperatures on the more open Rh surfaces (such as the Rh(100) surface), so it was possible that Rh adopts more active morphologies on reduced ceria.

Currently, there is still disagreement regarding NO surface structures on Rh(111), one concern being the failure to account for dissociated N and O atoms in the structural models. The actual transition in NO binding from 3-fold hollow to atop sites is also still not completely understood, as well as how the dissociation products affect this transition. In this paper, we describe studies using Auger electron spectroscopy (AES) and polarization modulation infrared reflection absorption spectroscopy (PM-IRAS) where we follow the structural transitions of NO on Rh(111) and the role of adsorbed oxygen and nitrogen in altering these structures. To our knowledge, these are the first experiments using the PM-IRAS technique at elevated pressures to study NO dissociation on the Rh(111) surface.

Experimental Procedures

The experimental apparatus used for these studies has been described in detail previously, so only a brief description will be given here.³⁵ All experiments were carried out in a stainless steel surface analysis apparatus consisting of two chambers. The main UHV chamber, with a base pressure of $<5 \times 10^{-10}$ Torr, is equipped for AES and LEED and also contains a mass spectrometer. Attached to the main chamber via a differentially pumped sliding seal is a high-pressure cell with CaF_2 windows for infrared studies. With the sample in the high-pressure cell, the pressure can be varied between 10^{-9} Torr and 1 atm with no disruption of the pumping in the main chamber. The Rh-(111) sample was spot-welded to a Ta wire, and the temperature was measured with a thermocouple spot-welded to the rear of the sample (Type C thermocouple: W-5%Re/W-26%Re). Using liquid nitrogen cooling and resistive heating, the temperature of the sample could be varied from 90 to 1250 K. Prior to performing experiments, the sample was oxidized at 650 K and then annealed at 1200 K to ensure cleanliness. Subsequent AES analysis showed that this procedure resulted in a sample free of carbon, sulfur, and oxygen. The PM-IRA spectra were obtained using a FTIR spectrometer coupled with a photoelastic modulator to subtract infrared signals arising from gas-phase absorption. Following reflection from the sample, the infrared beam passed through a demodulator/multiplexer, and the signal was collected using a mercury–cadmium–telluride (MCT) detector.

Results and Discussion

Figure 1 shows infrared spectra obtained at various temperatures after dosing 300 L (1×10^{-6} Torr s) for 300 s. Note that NO saturation occurs between 15 and 20 L. To ensure cleanliness of the sample, after each spectrum was acquired, the sample was flashed to 1200 K. AES analysis has shown that this procedure yields a clean surface. As can be seen, NO exposure below 150 K leads to a single vibrational mode at 1652 cm^{-1} . This mode was also observed by HREELS¹⁸ and assigned to NO bonding in 3-fold hollow sites.²⁶ However, at

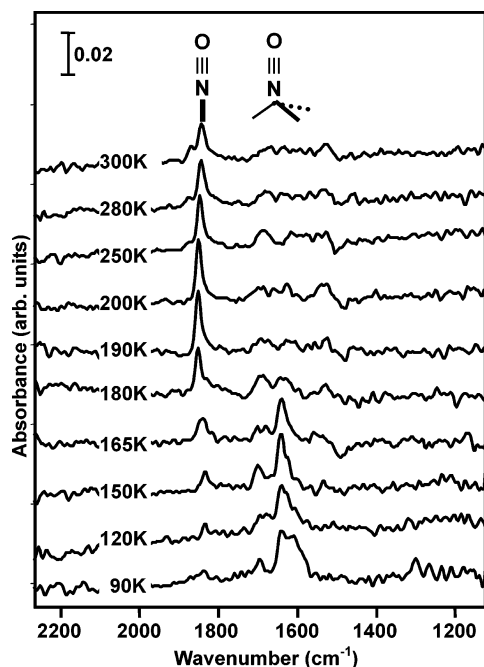


Figure 1. Temperature-dependent PM-IRA spectra of NO on Rh(111). A total of 300 L of NO was dosed at the indicated temperature, and the infrared spectrum was acquired. Prior to each dose and scan, the surface was flashed to 1200 K to remove any NO and its decomposition products.

approximately 150 K, a new feature appeared at 1848 cm^{-1} , corresponding to bonding at atop sites.^{18,26} With a further increase in the temperature, the intensity of this atop feature continued to increase, with a concomitant decrease in the hollow site feature. At 300 K, only the atop feature was evident. This change in the surface adsorption sites is common for CO adsorption on many metal surfaces with increasing CO coverages and also has been reported for NO adsorption.¹⁸ However, at adsorption temperatures below 150 K, only one mode, corresponding to NO at 3-fold hollow sites, is evident over the entire NO coverage range. These results suggest that the change of the NO adsorption site may be an activated process and/or associated with the decomposition of NO at elevated temperatures.

Next, experiments were carried out to determine the time-dependent nature of the PM-IRA spectra (Figure 2a). After exposing the Rh(111) surface to 20 L of NO (saturation coverage) at 250 K, spectra were acquired at 5 min intervals. The spectra are dominated by the 3-fold hollow feature at 1650 cm^{-1} , with a smaller feature at 1850 cm^{-1} related to atop NO. There are no apparent changes in the spectra after 25 min. However, a second 20 L of NO exposure (40 L total) leads to a noticeable change in the spectrum (Figure 2b). In this spectrum, the intensity of the atop feature approaches that of the 3-fold hollow site. Further exposure leads to an atop feature intensity greater than that of the 3-fold hollow feature (Figure 2c). Apparently, the addition of NO is a prerequisite for NO to bind at atop sites.

Further time-dependent experiments were carried out at 250 K under flowing conditions of 5×10^{-8} Torr NO. The spectra in Figure 3a are dominated initially by molecular NO binding at 3-fold hollow sites (1650 cm^{-1}). Bonding of NO at atop sites (1850 cm^{-1}) is also evident. However, with time, those features corresponding to 3-fold hollow sites disappear with the only significant feature in the spectrum being that due to molecular NO at atop sites. The changes in atop- and 3-fold hollow intensities as a function of time are summarized in Figure 3b.

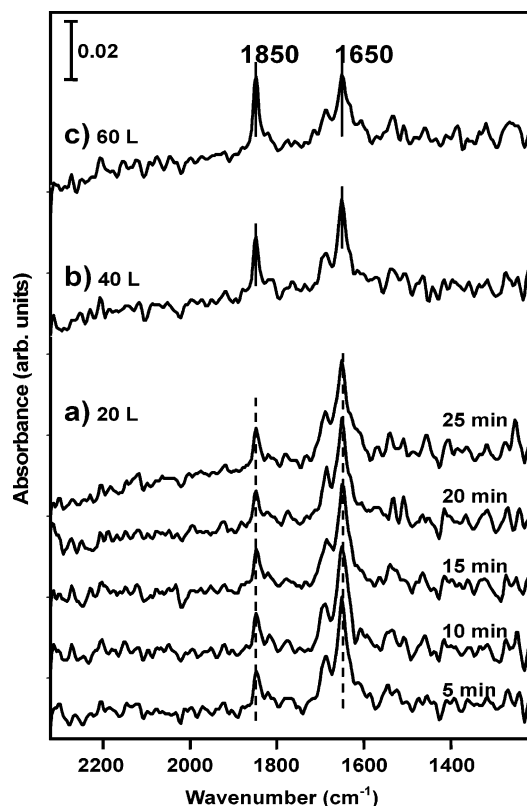


Figure 2. (a) PM-IRA spectra obtained after dosing 20 L of NO on the Rh(111) surface. Scans were then taken in 5 min intervals to observe any possible structural changes as a function of time. (b) Spectrum obtained following a 20 L dose (40 L total) of NO to the surface of panel a. (c) Spectrum was obtained following a final 20 L dose (60 L total) of NO to the surface of panel b.

Spectra were also acquired at 120 K after exposing the sample to 1×10^{-7} Torr NO as shown in Figure 4a. As expected at this temperature, 3-fold hollow bonding dominates the spectrum (Figure 4a1). With repeated flashing to 200 K in background NO (Figure 4a2 to a6), the atop feature grows, and the 3-fold hollow feature attenuates. These results are at odds with previous adsorption/dissociation mechanisms for NO on Rh(111)^{5,15,21,29} and offer further evidence that dissociation occurs at temperatures much lower than previously suggested. Note that similar experiments, where background NO is not present during the flash, lead to spectra where there is no change with respect to 3-fold hollow and atop bonding sites (Figure 4b). These results confirm that migration from 3-fold hollow sites does not occur during a vacuum anneal and that the atop bonding seen in Figure 4a is a result of the addition of gas-phase NO coadsorbed with NO decomposition species.

As mentioned in the Introduction, at the coverages reported previously, it is assumed that NO bonds molecularly since dissociation is not observed below 275 K.^{5,29} However, our results show that NO bonding occurs only at atop sites with the 3-fold hollow site being occupied only at relatively low temperatures (i.e., $<150\text{ K}$ (Figure 4)). The complete shift of the NO modes exclusively from 3-fold hollow to atop (Figures 1–4) cannot be explained based on the results and explanations previously reported (i.e., coverage-induced surface restructuring). The number of atop sites is identical to the 3-fold hollow sites, and also, NO prefers the 3-fold hollow sites at low NO coverage. These points suggest that dissociation of NO likely takes place below 200 K, much lower than the previous reported temperature of 275 K.^{5,29} The growth of the atop feature must result from the coadsorption of NO dissociation products that

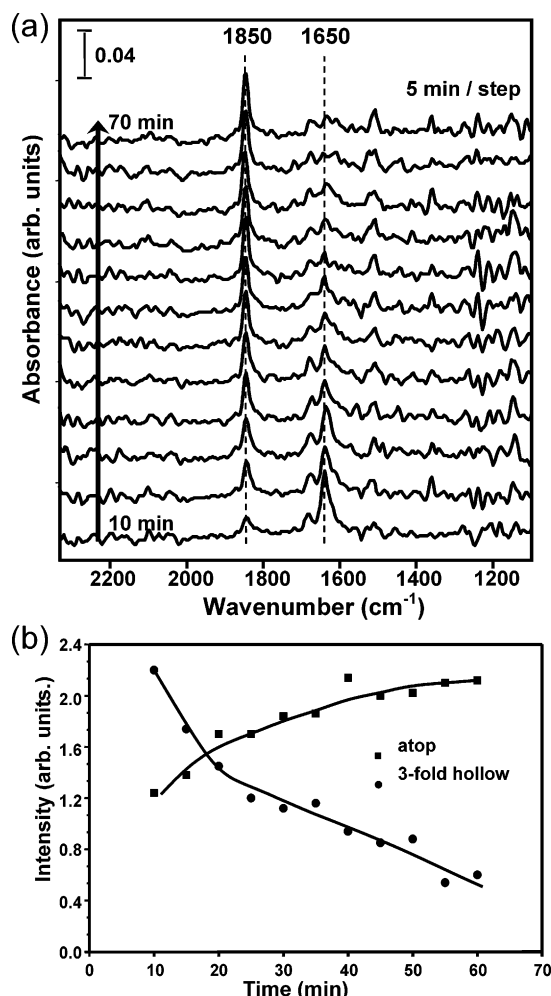


Figure 3. (a) Time-dependent NO adsorption at 250 K on Rh(111). The spectra were taken at 5 min intervals in 5×10^{-8} Torr flowing NO. (b) Plot showing the changes in the atop and 3-fold hollow site intensity from panel (a) as a function of time.

induces molecular NO at the atop site. Since the 3-fold hollow sites are filled with dissociation products (e.g. O_{ad}) as well as with molecular NO, incoming NO molecules are forced to adsorb at atop sites. Molecular NO is reported to desorb from the Rh(111) surface at approximately 400 K by TPD,^{5,21} so desorption can be ruled out as a cause for the decrease in the hollow-related IRAS feature. The only other possibilities are the movement of NO from the hollow sites to the atop sites or the dissociation of the NO molecules adsorbed at the 3-fold hollow sites. It is unlikely that NO migrates from the hollow sites, as the time lapse experiments at 250 K show (Figure 2a). Therefore, a plausible explanation is that the molecules in the hollow sites are dissociating and filling the hollow sites. The data of Figure 2b,c support this conclusion, as further exposure of the surface to NO leads to the population of atop sites. This explanation is the only one that can account for the changes seen in the spectra; however, it is at odds with all previous work, in which dissociation is inhibited at relative high NO coverages.^{5,15,21,29}

To examine how the NO dissociation products influence bonding, NO was dosed on an oxygen pretreated surface at 120 K (Figure 5). On an oxygen-free surface, NO adsorbed only at 3-fold hollow sites (Figure 5a). However, on a surface pretreated with various amounts of oxygen (i.e., 2, 4, and 6 L at 650 K) atop NO adsorption was also observed, with the intensity increasing with an increase in the O_2 coverage and a concomitant

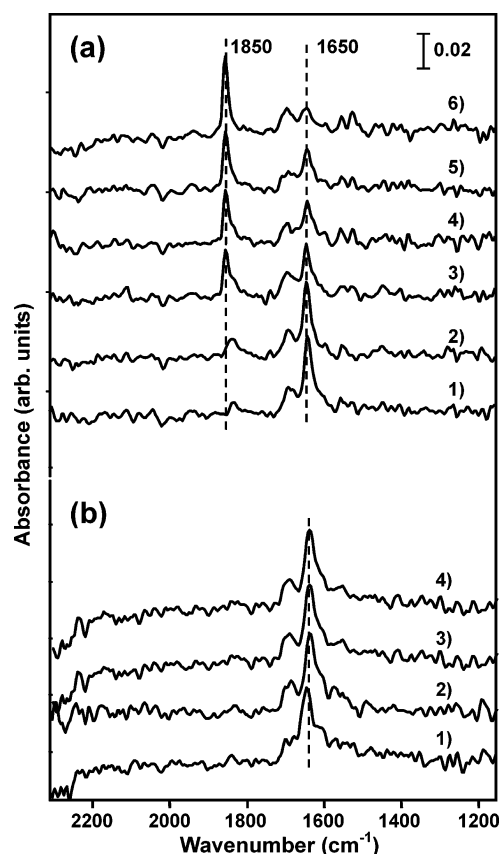


Figure 4. (a1) Spectrum obtained after exposing the Rh(111) sample to 1×10^{-7} Torr NO while scanning. (a2 to a6) Spectra obtained after flashing the sample to 200 K and cooling in 1×10^{-7} Torr NO. (b1) Spectrum obtained after exposing the Rh(111) sample to 1×10^{-7} Torr NO while scanning. (b2 to a4) Spectra obtained after flashing the sample to 200 K. All spectra were obtained at 150 K.

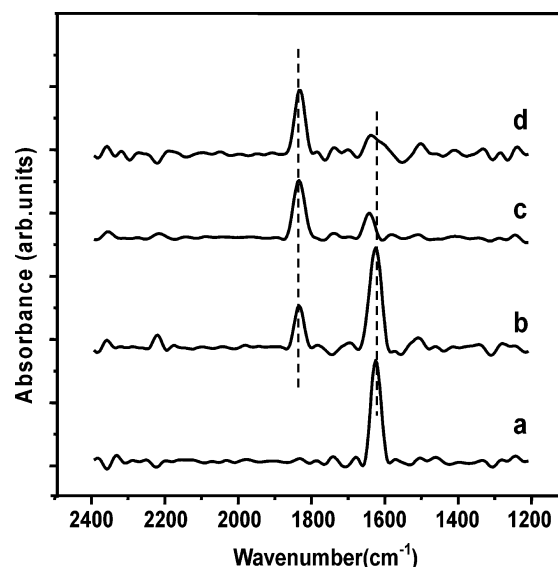


Figure 5. 2 L NO adsorption at 120 K on Rh(111) pretreated with various coverages of oxygen at 650 K obtained by dosing: (a) 0 L of O_2 ; (b) 2 L of O_2 ; (c) 4 L of O_2 ; and (d) 6 L of O_2 .

decrease in the intensity of 3-fold hollow NO sites. These data confirm that surface oxygen leads to NO adsorption at atop sites, suggesting that NO and oxygen coexist in the same phase, in contrast to a previous proposal, based on STM data, that NO and oxygen form separate phases on the surface.⁷

These data have important implications for understanding how NO interacts with Rh(111). It is shown that at room temperature

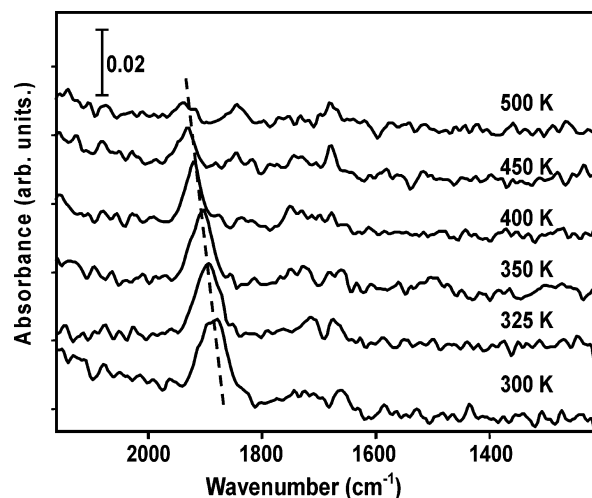


Figure 6. PM-IRAS spectra obtained as a function of temperature in the presence of 1 Torr NO. The Rh(111) sample was exposed to 1 Torr NO at 300 K, and the temperature was then raised as indicated.

or even below, the surface is essentially covered by atop NO, with very little 3-fold hollow site occupation. This contrasts with previous reports, particularly those surface adsorbate structures^{16,23,24,26} with at least a 2:1 ratio of atop/hollow or hollow/atop. Since NO dissociation has received considerable attention on this surface, it is surprising that the dissociation products, O_{ad} and N-containing species, have not been considered with respect to their influence on the structures of NO on Rh. Although the surface structure at room temperature is purported to change at elevated (~ 1 Torr) pressure,²³ we note that our results for 1 Torr NO on Rh(111) show that the surface is essentially covered by atop NO (Figure 6). The present study strongly suggests that further theoretical and experimental studies should be carried out to clarify the remaining discrepancies in this important adsorbate system.

Acknowledgment. We acknowledge with pleasure the support of this work by the Department of Energy, Office of Basic Energy Sciences, Division of Chemical Sciences and the Robert A. Welch Foundation.

References and Notes

- (1) Paul, J.-F.; Perez-Ramirez, J.; Ample, F.; Ricart, J. M. *J. Phys. Chem. B* **2004**, *108*, 17921–17927.
- (2) Zaera, F.; Gopinath, C. S. *Chem. Phys. Lett.* **2000**, *332*, 209–214.
- (3) Avalos, L.; Bustos, V.; Unac, R.; Zaera, F.; Zgrablich, G. *J. Mol. Catal.* **2005**, *228*, 89–95.
- (4) Peden, C. H. F.; Goodman, D. W.; Blair, D. S.; Berlowitz, P. J.; Fisher, G. B.; Oh, S. H. *J. Phys. Chem.* **1988**, *92*, 1563–1567.
- (5) Borg, H. J.; Reijerse, J. F.; C.-J., M.; van Santen, R. A.; Niemantsverdriet, J. W. *J. Chem. Phys.* **1994**, *101*, 10052–10063.
- (6) Hopstaken, M. J. P.; Niemantsverdriet, J. W. *J. Phys. Chem. B* **2000**, *104*, 3058–3066.
- (7) Xu, H.; Ng, K. Y. S. *Surf. Sci.* **1996**, *365*, 779–788.
- (8) Kim, Y. J.; Thevuthasan, S.; Herman, G. S.; Peden, C. H. F.; Chambers, S. A.; Belton, D. N.; Permana, H. *Surf. Sci.* **1996**, *359*, 269–279.
- (9) Papapolymerou, G. A.; Schmidt, L. D. *Langmuir* **1985**, *1*, 488–495.
- (10) Janssen, N. M. H.; Cholach, A. R.; Ikai, M.; Tanaka, K.; Nieuwenhuys, B. E. *Surf. Sci.* **1997**, *382*, 201–213.
- (11) Schmatloch, V.; Jirka, I.; Kruse, N. *J. Chem. Phys.* **1994**, *100*, 8471–8482.
- (12) Dubois, L. H.; Hansma, P. K.; Somorjai, G. A. *J. Catal.* **1980**, *65*, 318–327.
- (13) Baird, R. J.; Ku, R. C.; Wynblatt, P. *Surf. Sci.* **1980**, *97*, 346–362.
- (14) Wolf, R. M.; Bakker, J. W.; Nieuwenhuys, B. E. *Surf. Sci.* **1991**, *246*, 135–140.
- (15) DeLouise, L. A.; Winograd, N. *Surf. Sci.* **1985**, *159*, 199–213.
- (16) Loffreda, D.; Simon, D.; Sautet, P. *J. Catal.* **2003**, *213*, 211–225.
- (17) Castner, D. G.; Sexton, B. A.; Somorjai, G. A. *Surf. Sci.* **1978**, *71*, 519–540.
- (18) Kao, C.-T.; Blackmon, G. S.; Hove, M. A. V.; Somorjai, G. A. *Surf. Sci.* **1989**, *224*, 77–96.
- (19) Zasada, I.; Hove, M. A. V.; Somorjai, G. A. *Surf. Sci.* **1998**, *418*, L89–L93.
- (20) Root, T. W.; Schmidt, L. D.; Fisher, G. B. *Surf. Sci.* **1983**, *134*, 30–45.
- (21) Root, T. W.; Fisher, G. B.; Schmidt, L. D. *J. Chem. Phys.* **1986**, *85*, 4679–4686.
- (22) Root, T. W.; Fisher, G. B.; Schmidt, L. D. *J. Chem. Phys.* **1986**, *85*, 4687–4695.
- (23) Rider, K. B.; Hwang, K. S.; Salmeron, M.; Somorjai, G. A. *Phys. Rev. Lett.* **2001**, *86*, 4330–4333.
- (24) Rider, K. B.; Hwang, K. S.; Salmeron, M.; Somorjai, G. A. *J. Am. Chem. Soc.* **2002**, *124*, 5588–5593.
- (25) Zhdanov, V. P.; Kasemo, B. *Surf. Sci. Rep.* **1997**, *29*, 31–90.
- (26) Loffreda, D.; Simon, D.; Sautet, P. *Chem. Phys. Lett.* **1998**, *291*, 15–23.
- (27) Mavrikakis, M.; Rempel, J.; Greeley, J.; Hansen, L. B.; Norskov, J. K. *J. Chem. Phys.* **2002**, *117*, 6737–6744.
- (28) Inderwildi, O. R.; Lebedez, D.; Deutschmann, O.; Warnatz, J. *J. Chem. Phys.* **2005**, *122*, 154702.
- (29) Hermse, C. G. M.; Frechard, F.; van Bavel, A. P.; Lukkien, J. J.; Niemantsverdriet, J. W.; van Santen, R. A.; Jansen, A. P. *J. Chem. Phys.* **2003**, *118*, 7081–7089.
- (30) Overbury, S. H.; Mullins, D. R.; Kundakovic, L. *Surf. Sci.* **2001**, *470*, 243–254.
- (31) Mullins, D. R.; Overbury, S. H. *Surf. Sci.* **2002**, *511*, L293–L297.
- (32) Ferrizz, R. M.; Egami, T.; Wong, G. S.; Vohs, J. M. *Surf. Sci.* **2001**, *476*, 9–21.
- (33) Granger, P.; Praliaud, H.; Billy, J.; Leclercq, L.; Leclercq, G. *Surf. Interface Anal.* **2002**, *34*, 92–96.
- (34) Matsushima, T.; Rzeznicka, I.; Ma, Y. H. *Chem. Rec.* **2005**, *5*, 81–93.
- (35) Ozensoy, E.; Meier, D. C.; Goodman, D. W. *J. Phys. Chem. B* **2002**, *106*, 9367–9371.